The mechanism study on transport properties in perovskite oxide *p-n* junctions

Peng Han, Kui-juan Jin,[a] Hui-bin Lu, Qing-Li Zhou, Yue-Liang Zhou, and Guo-Zhen Yang
Beijing National Laboratory for Condensed Matter Physics, Institute of Physics, Chinese Academy of Sciences, Beijing 100080, China

(Received 24 September 2007; accepted 11 October 2007; published online 30 October 2007)

The drift-diffusion mechanism, the interband Zener tunneling theory, and the trap assisted tunneling model are combined to reveal the transport properties in a multicorrelated system of the p-$La_{0.9}Sr_{0.1}MnO_3$/n-$SrNb_{0.01}Ti_{0.99}O_3$ junction with various temperatures. The good agreement between the calculated and measured I-V curves reveal that the drift-diffusion mechanism dominates the transport process with forward bias, and the interband Zener tunneling plays an important role for the carrier transport with high reverse bias. In the low reverse bias, the I-V characteristic of oxide device is mainly attributed to the trap assisted tunneling process caused by the oxygen vacancy induced states. © *2007 American Institute of Physics*.
[DOI: 10.1063/1.2804608]

The immense interesting phenomena of the correlated electron perovskite oxide material, such as colossal magnetoresistance (CMR) effect and picosecond photoelectric characteristic, have provided the impetus for fabricating the perovskite oxide devices, including field-effect transistors,[1] manganite tunnel junctions,[2] and *p-n* junctions.[3–5] Recently, many novel phenomena such as unusual CMR, photovoltaic, and ferroelectricity effects have been observed in these devices.[1–7] Although the vigorous experimental and theoretical researches[8–10] have been carried out in the perovskite oxide system, a detailed understanding of this kind of material is still unknown due to the complicated interplay of spin, charge, and orbital coupling and the competition of energy scales.[2] Furthermore, it was believed that the band theory for semiconductor *p-n* junctions would be difficult to apply to the correlated oxide devices due to the Coulomb repulsion among electrons.[3] In addition, different from the conventional semiconductors, the oxygen vacancies can be generated in the perovskite oxide material due to lack of oxygen. The role of these oxygen vacancies placed in the transport property has not been known clearly. Therefore, a proper theoretical method to accurately reveal the transport process in the perovskite oxide devices is fundamentally important.

Different from the strong-correlated perovskite oxide, the hole-doped $La_{0.9}Sr_{0.1}MnO_3$ is a multicorrelated ferromagnetic semiconductor.[3,11] The Coulomb repulsion among electrons in the multicorrelated system is much weaker than that in the strong-correlated system, and this provides the possibility to analyze the transport characteristics of multicorrelated devices by using the semiconductor band theory. However, few numerical studies have been focused on the transport process in the oxide devices by using the semiconductor theory until now. In our previous work, a numerical simulation of the transport properties in a homogeneous $SrTiO_3$ *p-n* junction with forward bias has been carried out recently.[12] The self-consistent study of transport property in a perovskite oxide *heterostructure* with both forward and *reverse* bias has never been reported. In addition, the theoretical analysis of the mechanism of the leakage current in the oxide *p-n* junction is still lacking either.

In this work, we analyze the transport properties at the interface region of the perovskite oxide heterojunction of $La_{0.9}Sr_{0.1}MnO_3$/$SrNb_{0.01}Ti_{0.99}O_3$ (LSMO/SNTO) self-consistently based on Poisson equation, and the drift-diffusion formulation with considering Richardson current at the interface over a wide range of bias and taking into account the effects of trap assisted tunneling and interband Zener tunneling processes at the reverse bias. Under the applied bias voltage, the I-V characteristics, the band structures, the electric fields, and the carrier concentrations at the interface region of the LSMO/SNTO heterostructure are obtained with various temperatures. Our results reveal that the drift-diffusion process is the dominative transport mechanism in the oxide heterostructure with forward bias, and the interband Zener tunneling current plays an important role for the reversed transport process with high reverse bias. In addition to the conventional semiconductor theory, the trap assisted tunneling process assisted by the oxygen vacancy-induced states in the forbidden gap[13] is proved to be the main mechanism for the leakage current in the oxide *p-n* junction at low reverse bias.

In the conventional transport theory of semiconductors, the current transport across the heterojunction interface is taken into account by employing the Richardson thermionic emission current at the interface, as well as the drift-diffusion current is used in the homogeneous regions.[14] The behavior of electrostatic potential $\phi(x)$, electrons $n(x)$, and holes $p(x)$ under the external bias voltage V_{bias} are obtained by solving the following coupled equations self-consistently.

$$-\frac{d^2\phi(x)}{dx^2}=\frac{q}{\varepsilon}[p(x)-n(x)-N_a+N_d],$$

$$D_n\frac{d^2n(x)}{dx^2}-\mu_n\frac{d\phi(x)}{dx}\frac{dn(x)}{dx}-\mu_n n(x)\frac{d^2\phi(x)}{dx^2}=R(x),$$

[a]Electronic mail: kjjin@aphy.iphy.ac.cn.

 © 2007 American Institute of Physics

$$D_p\frac{d^2p(x)}{dx^2}+\mu_p\frac{d\phi(x)}{dx}\frac{dp(x)}{dx}+\mu_p p(x)\frac{d^2\phi(x)}{dx^2}=R(x), \quad (1)$$

where q is the electron charge, ε is the dielectric permittivity, D_n and μ_n (or D_p and μ_p) are the electron (or hole) diffusion coefficient and mobility, respectively, N_a is the ionized acceptor density in p region, and N_d is the ionized donor density in n region. $R(x)$ is the recombination rate of the Shockley-Read-Hall recombination process.[14] The boundary conditions of Poisson equation are set to be 0 and V_d-V_{bias} at the p and n side far away from the space charge region, where V_d denotes the build-in potential. The boundary conditions for the concentration of hole and electron at the p (or n) side are N_a [or $n_i^2(L)/N_d$] and $n_i^2(0)/N_a$ (or N_d), respectively. $n_i(0)$ and $n_i(L)$ are the intrinsic concentration in the p and n regions, respectively.

With an applied reverse-bias voltage, electrons in the valence band on the p side can directly tunnel to the empty states in the n side with energy between E_{vp} and E_{Fn}, where, E_{vp} is the top of valence band in the homogeneous region of the p side and E_{Fn} is the Fermi level in the homogeneous region of the n side. Because the width of barrier between the valence band of p side and the conduction band of n side decreases with the increase of reverse bias voltage, the tunneling current increases rapidly with reverse-bias voltage. The interband Zener tunneling current density is calculated by using the method given in Ref. 15.

Different from the conventional semiconductors, it is experimentally known that the oxygen content of oxide materials can be changed depending on the film growth parameters and postdeposition treatment, leading to the likely formation of oxygen vacancies. Recently, Picozzi *et al.* demonstrated that the oxygen vacancy can induce states in the forbidden gap of LSMO based on their *ab initio* calculation.[13] Thus, a two-step tunneling process via traps generated by the oxygen vacancy-induced states (the so-called trap assisted tunneling) should be considered in the transport process in the oxide p-n junctions with reverse bias.[17–19] The trap assisted tunneling process has attracted much attention over many years, and several authors have proposed theoretical models to describe it.[17–19] Among them, the model proposed by Suzuki *et al.*[19] is well accepted. In our work, this model[19] is employed to describe the trap assisted tunneling process in the oxide p-n junction with reverse bias. The trap assisted tunneling current J_{TAT} can be calculated as

$$J_{\text{TAT}}=qN_t\sigma_t\int_{E_{\text{Fn}}}^{E_{\text{vp}}}N(E)F(E)\frac{T_1(E)T_2(E)}{T_1(E)+T_2(E)}dE, \quad (2)$$

where $N(E)$ denotes the density of state and $F(E)$ describes the Fermi distribution function. N_t presents the density of traps and σ_t is the effective capture cross section. The values of $N_t\sigma_t$ are taken as 0.15, 0.75, and 1.0 at $T=190$, 255, and 190 K, respectively. The tunneling rates of this two-step process $T_1(E)$ and $T_2(E)$ are obtained with the method given in Ref. 15.

With these formulas, we have performed a self-consistent calculation on the transport properties in the oxide p-n junction of LSMO/SNTO over a wide range of the bias voltages. The concentrations of the acceptor and the donor are $N_a=4.0\times10^{19}$ cm^{-3} and $N_d=1.63\times10^{20}$ cm^{-3}, respectively. The other necessary parameters for our calculation can be found in Table I.

TABLE I. Material parameters used in the calculation (Refs. 6 and 16).

Parameters	LSMO	SNTO
Band gap E_g (eV)	0.8	2.8
Affinity energy χ (eV)	3.95	4.05
Dielectric constant ε (ε_0)	10.0	300.0
Electron mobility μ_n (cm^2/V s)	10.0	8.0
Hole mobility μ_p (cm^2/V s)	1.8	0.1

The calculated band structure of LSMO/SNTO p-n junction without bias voltage is shown in Fig. 1. In this figure, the space charge region locates mostly at the n region of SNTO even though the doping density of SNTO is greater than that of LSMO. This is due to the high dielectric constant of SNTO material. To study the mechanism of transport process in the oxide p-n junction, we plot the I-V curves of the interband Zener tunneling process (solid curve), the trap assisted tunneling process (dashed curve), the combined theoretical results (dotted curve), and the experimental ones (hollow squares) with $T=190$, 255, and 290 K in Fig. 2(a)–2(c), respectively. The experimental data are obtained from the recent work of our group.[5,6] As shown in these figures, the good agreement between the theoretical and experimental data with forward bias proves that the drift-diffusion model can be employed to describe the forward transport process in the oxide heterostructure. For the case of reverse bias, the theoretical results reveal that the trap assisted tunneling process, which should be assisted by the oxygen vacancy induced states, is the dominant transport mechanism for the transport process in the oxide p-n junction. In addition to the leakage current caused by the trap assisted tunneling, the interband Zener tunneling is also important for the transport process with reverse bias. As shown in Fig. 2, the interband Zener tunneling currents are increased with the increase of bias voltage and the decrease of temperature. Thus, this process plays a more important role for the transport process with higher reverse bias at low temperature in the oxide p-n junction system.

In summary, the transport properties in the multicorrelated electron oxide heterojunction have been systemically

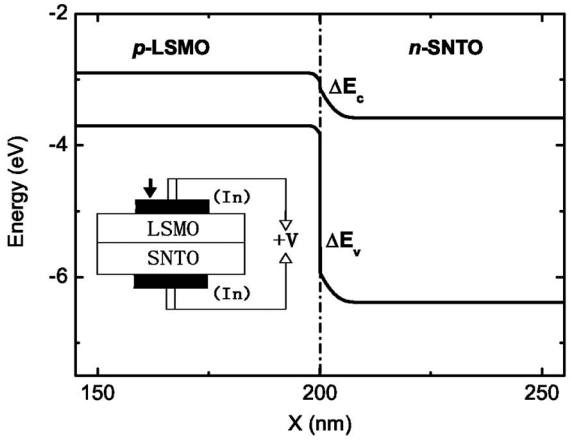

FIG. 1. The band-energy profile of the $La_{0.9}Sr_{0.1}MnO_3/SrNb_{0.01}Ti_{0.99}O_3$ heterojunction with no bias applied across the entire system. The inset is a schematic illustration of the p-n junction sample.

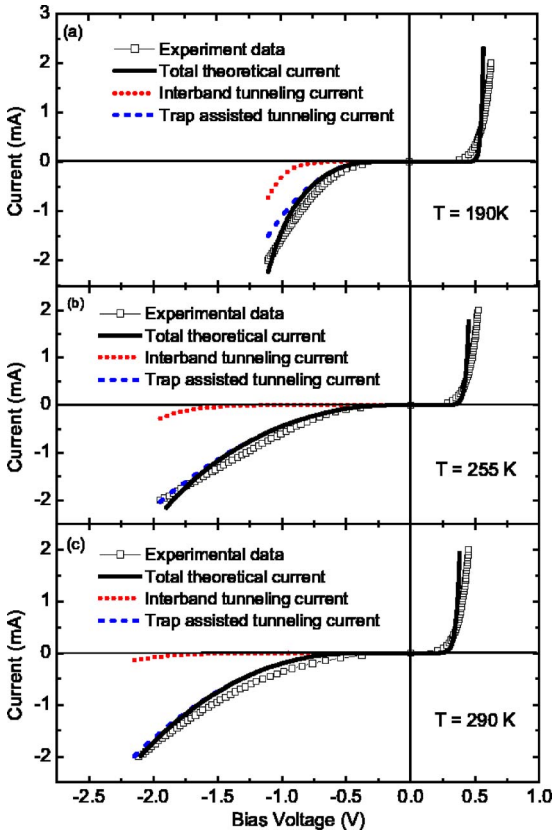

FIG. 2. (Color online) The theoretical results vs experimental data from reverse bias to forward bias with (a) $T=190$ K, (b) $T=255$ K, and (c) $T=290$ K, respectively. In these figures, the solid, dashed, and dotted curves represent the interband, Zener tunneling current, trap assisted tunneling current, and total theoretical current, respectively. The hollow squares describe the experimental data.

studied based on the self-consistent calculation over a wide range of applied voltages with various temperatures. The good agreement between theoretical results and experimental data proves that the drift-diffusion model is a good method to analyze the forward transport process in the perovskite oxide *p-n* junctions. For the case of low reverse bias, the transport characteristic is mainly determined by the trap assisted tunneling phenomenon assisted by the oxygen vacancy induced states. In the higher reverse bias, the interband Zener tunneling is the dominate transport mechanism for the oxide devices. This work will benefit to the further study of analyzing the spin polarization transport phenomena and picosecond photoelectric characteristic in the all-oxide devices.

This work was supported by the National Natural Science Foundation of China (10674164) and the National Basic Research Program of China.

[1]D. M. Newns, J. A. Misewich, C. C. Tsuei, A. Gupta, B. A. Scott, and A. G. Schrott, Appl. Phys. Lett. **73**, 780 (1998); J. A. Misewich and A. G. Schrott, *ibid.* **76**, 3632 (2000).
[2]C. Mitra, P. Raychaudhuri, K. Dörr, K. H. Muller, L. Schultz, P. M. Oppeneer, and S. Wirth, Phys. Rev. Lett. **90**, 017202 (2003); C. Mitra, P. Raychaudhuri, G. Kobernik, K. H. Muller, L. Schultz, and R. Pinto, Appl. Phys. Lett. **79**, 2408 (2001); J. O'Donnell, A. E. Andrus, S. Oh, E. V. Colla, and J. N. Eckstein, *ibid.* **76**, 1914 (2000).
[3]H. Tanaka, J. Zhang, and T. Kawai, Phys. Rev. Lett. **88**, 027204 (2002).
[4]A. Tiwari, C. Jin, D. Kumar, and J. Narayan, Appl. Phys. Lett. **83**, 1773 (2004).
[5]H. B. Lu, G. Z. Yang, Z. H. Chen, S. Y. Dai, Y. L. Zhou, K. J. Jin, B. L. Cheng, M. He, L. F. Liu, H. Z. Guo, Y. Y. Fei, W. F. Xiang, and L. Yan, Appl. Phys. Lett. **84**, 5007 (2004); H. B. Lu, S. Y. Dai, Z. H. Chen, Y. L. Zhou, B. L. Cheng, K. J. Jin, L. F. Liu, G. Z. Yang, and X. L. Ma, *ibid.* **86**, 032502 (2005).
[6]K.-j. Jin, H.-b. Lu, Q.-l. Zhou, K. Zhoa, B.-l. Cheng, Z.-h. Chen, Y.-l. Zhou, and G.-Z. Yang, Phys. Rev. B **71**, 184428 (2005).
[7]C. M. Xiong, Y. G. Zhao, B. T. Xie, P. L. Lang, and K. J. Jin, Appl. Phys. Lett. **88**, 193507 (2006); Y. Huang, K. Zhao, H. B. Lu, K.-j. Jin, M. He, Z. H. Chen, Y. L. Zhou, and G. Z. Yang, *ibid.* **88**, 061919 (2006).
[8]P. Mandal and S. Das, Phys. Rev. B **56**, 15073 (1997).
[9]C. Mitra, P. Raychaudhuri, J. John, S. K. Dhar, A. K. Nigam, and R. Pinto, J. Appl. Phys. **89**, 524 (2001).
[10]C. Zener, Phys. Rev. **82**, 403 (1951); J. B. Goodenough, *ibid.* **100**, 564 (1955); P. W. Anderson and H. Hasegawa, *ibid.* **100**, 675 (1955).
[11]E. Dagotto, T. Hotta, and A. Moreo, Phys. Rep. **344**, 1 (2001).
[12]Q.-l. Zhou, K.-j. Jin, H.-b. Lu, P. Han, Z.-h. Chen, K. Zhao, Y.-l. Zhou, and G.-z. Yang, Europhys. Lett. **71**, 283 (2005).
[13]S. Picozzi, C. Ma, Z. Yang, R. Bertacco, M. Cantoni, D. Petti, S. Brivio, and F. Ciccacci, Phys. Rev. B **75**, 094418 (2007).
[14]K. Horio and H. Yanai, IEEE Trans. Electron Devices **37**, 1093 (1990); K. Yang, J. R. East, and G. I. Haddad, IEEE Trans. Electron Devices **41**, 138 (1994); K. Yang, J. R. East, and G. I. Haddad, Solid-State Electron. **36**, 321 (1993); P. Han, K.-j. Jin, Y. Zhou, X. Wang, Z. Ma, S. F. Ren, A. G. Mal'shukov, and K. A. Chao, J. Appl. Phys. **99**, 074504 (2006).
[15]O. Pinaud, J. Appl. Phys. **92**, 1987 (2002); A. El. Ayyadi and A. Jüngel, SIAM J. Appl. Math. **66**, 554 (2006).
[16]S. Myhajlenko, A. Bell, F. Ponce, J. L. Edward, Jr., Y. Wei, B. Craigo, D. Convey, H. Li, R. Liu, and J. Kulik, J. Appl. Phys. **97**, 014101 (2005); R. Moos and K. H. Härdtl, *ibid.* **80**, 393 (1996); S. Chambers, Y. Liang, Z. Yu, R. Droopad, J. Ramdani, and K. Eisenbeiser, Appl. Phys. Lett. **77**, 1662 (2000).
[17]R. Perera, A. Ikeda, R. Hattori, and Y. Kuroki, Microelectron. Eng. **65**, 357 (2003).
[18]M. P. Houng, Y. H. Wang, and W. J. Chang, J. Appl. Phys. **86**, 1488 (1999), and references therein.
[19]E. Suzuki, D. K. Schroder, and Y. Hayashi, J. Appl. Phys. **60**, 3616 (1986).